

## Propagation of single-cycle pulsed light beams in dispersive media

Miguel A. Porras\*

*Departamento de Física Aplicada, Escuela de Ingenieros de Minas, Universidad Politécnica de Madrid, Ríos Rosas 21, E-28003 Madrid, Spain*

(Received 7 June 1999)

We describe a family of solutions of the three-dimensional envelope equation in dispersive media beyond the slowly varying envelope approximation [T. Brabec *et al.*, Phys. Rev. Lett. **78**, 3282 (1997)] that represents few-cycle pulsed light beams evolving due to gain (losses), phase and gain dispersion, diffraction, and space-time focusing. We then show that group velocity dispersion tends to bend the propagating pulse front, in the same sense as diffraction in anomalous dispersion, and in the opposite sense in normal dispersion. In the latter case, the diffraction-induced pulse front curvature and the associated pulse broadening can be eliminated along the whole propagation by setting the diffraction length equal to the dispersion length. Simple analytic expressions for these dispersion-diffraction coupled effects are given. [S1050-2947(99)08912-X]

PACS number(s): 42.65.Re, 42.65.Sf, 42.25.Bs, 42.60.Jf

### I. INTRODUCTION

The present investigation is concerned with the propagation of narrow light beams of a few femtoseconds of duration in dispersive media. The rapid development of methods of pulse compression have made the experimental production of such ultrashort few-cycle, even single-cycle, pulses feasible. For this reason, much attention is being paid to their propagation in vacuum, linear and nonlinear media, and optical systems.

In this sense, it has been shown [1] that the useful concepts of carrier frequency and envelope can be extended down to the limit of single-cycle pulses. The usual first-order envelope equation within the slowly-varying-envelope approximation (SVEA), however, fails at describing their propagation [2–4]. The lack of an appropriate envelope propagation equation for single-cycle pulses appears now to be resolved with the recent derivation of an extended nonlinear envelope equation [1], which is valid within a wider frame called the slowly-evolving-wave approximation (SEWA). This envelope equation incorporates, together with the effects of dispersion and nonlinearity, the unavoidable effects of diffraction [5] and space-time focusing, [2] or the dependence of diffraction with frequency, in the propagation of few-cycle pulses.

On the other hand, the diffraction of few-cycle pulses in vacuum has been studied for some time [6]. Due to the superbroad spectra of these pulses, the different spectral components also diffract differently. In the space-time domain, this results in some diffraction-induced transformations of the temporal form of the pulse (otherwise undeformable), which include pulse polarity reversal [7], time differentiation on propagation [5], pulse broadening, and redshift of the spectrum along each beam cross section [6,8]. Diffraction is also responsible for an increasing pulse front curvature [8] on propagation due to the time delay of arrival between different parts of the pulse at each cross section [8,6,9]. In practice, the net effect of this curvature is an increase of the

pulse duration in a large area receiver.

In this paper, we develop a method to obtain physically meaningful, few-cycle, beamlike solutions of the three-dimensional linear SEWA envelope equation, from the unphysical few-cycle solutions of the one-dimensional SVEA equation. These ultrashort pulsed-beam solutions propagate under the coupled effects of gain (absorption), phase and gain dispersion of any order, and diffraction, with the proper inclusion of space-time focusing.

The aforementioned diffraction-induced phenomena in vacuum are also encountered in the solutions of the SEWA envelope equation in dispersive media. Moreover, we find, as a phenomenon peculiar to dispersive propagation of ultrashort pulsed beams, an additional dispersion-induced pulse front curvature which may enhance, reverse, or suppress the diffraction curvature along the entire propagation of the pulsed beam. The suppression of the curvature, and therefore of the associated pulse broadening, occurs with normal group velocity dispersion (GVD) when the strengths of diffraction and dispersion, measured by their characteristic axial length scales of interaction, are similar. This can be qualitatively understood as a dispersive compensation of the diffraction-induced propagation path difference between the more tilted low-frequency components of the spectrum and the less tilted high-frequency components, in a similar way that adequate dispersive optical elements have been developed [10] to avoid pulse front distortion due to path differences in the focusing of ultrashort pulses by lenses [11].

### II. ULTRASHORT PULSED-BEAM PROPAGATION EQUATION BEYOND THE SVEA

The propagation of an electromagnetic wave in a linear dispersive medium can be described by the wave equation

$$\Delta E(\mathbf{r}, t) - \frac{1}{c^2} \partial_t^2 \int_{-\infty}^t dt' \varepsilon(t-t') E(\mathbf{r}, t') = 0, \quad (1)$$

where  $\varepsilon(t) = (1/2\pi) \int_{-\infty}^{\infty} \varepsilon(\omega) \exp(-i\omega t)$ , and  $\varepsilon(\omega)$  is the electric permittivity of the medium. For the carrier-enveloped field  $E(\mathbf{r}, t) = A(\mathbf{r}, t) \exp(-i\omega_0 t + i\beta_0 z)$ , with  $\beta_0$

\*Electronic address: porras@dfarn.upm.es

=Re[ $k(\omega_0)$ ],  $k(\omega) = (\omega/c)\sqrt{\varepsilon(\omega)}$ , and for pulses as short as a single optical period,  $\Delta t = T_0 = 2\pi/\omega_0$ , the following first-order envelope equation has been derived recently [1]:

$$\partial_{\xi} A = \left( -\frac{\alpha_0}{2} + iD \right) A + \frac{i}{2\beta_0} \left( 1 + i\frac{\beta_1}{\beta_0} \partial_{\tau} \right)^{-1} \Delta_{\perp} A, \quad (2)$$

where  $\Delta_{\perp} = \partial_x^2 + \partial_y^2$ ,  $\tau = t - \beta_1 z$ ,  $\xi = z$ ,  $\beta_m = \text{Re}[\partial_{\omega}^m k(\omega)|_{\omega_0}]$ ,  $\alpha_m = 2 \text{Im}[\partial_{\omega}^m k(\omega)|_{\omega_0}]$ , and

$$D = -\frac{\alpha_1}{2} \partial_{\tau} + \sum_{m=2}^{\infty} \frac{\beta_m + i\alpha_m/2}{m!} (i\partial_{\tau})^m \quad (3)$$

is the dispersion operator. [Throughout this paper, the symbols  $\Delta t$  and  $\Delta\omega$  without any subscript stand for the full width at half maximum (FWHM) of  $|A|^2$  and its Fourier transform  $|\hat{A}|^2$ .]

The validity of Eq. (2) is restricted by the condition [1]

$$|\partial_{\xi} A| \ll \beta_0 |A|, \quad (4)$$

which requires a small change of the envelope  $A$  as the pulse covers a distance equal to the wavelength  $2\pi/\beta_0$ . In Brabec's derivation [1] of Eq. (2), the quotient  $\beta_1/\beta_0$  is next replaced with  $1/\omega_0$  and the difference is neglected, under the additional condition  $v_f \approx v_g$ , where  $v_f = \omega_0/\beta_0$  and  $v_g = \beta_1^{-1}$  are the phase and group velocities, respectively, at the carrier frequency [1]. Although the numerical differences will be negligible in most cases, Eq. (2) without this approximation will yield (as we shall see) more consistent analytic expressions, at least for linear propagation. Space-time focusing is included in Eq. (2) in its lowest order, as defined in the original reference [2], whereas in the SEWA equation this lowest order is slightly falsified. For clarity, we shall refer to Eq. (2) under the only condition (4) as the linear envelope equation under the slowly-evolving-envelope approximation (SEEA). On removing the condition  $v_f \approx v_g$  on the material medium, this SEEA equation applies under the same requirements for the material medium, implicit in the condition (4), as the usual SVEA equation but retains, at the same time, its validity down to single-cycle pulses.

### III. PULSED GAUSSIAN BEAM SOLUTION OF THE SEEA ENVELOPE EQUATION

Searching for solutions of Eq. (2), we multiply by  $[1 + i(\beta_1/\beta_0)\partial_{\tau}]$ , Fourier transform the equation, and make the change  $\hat{A} = \hat{A}' \exp[(-\alpha_0/2 + i\hat{D})\xi]$ , where  $\hat{A}'(\omega - \omega_0)$  and  $\hat{D}(\omega - \omega_0)$  are the temporal Fourier transforms of  $A$  and the operator  $D$ , respectively. We then obtain the usual equation for paraxial diffraction,

$$\Delta_{\perp} \hat{A}' + 2i\beta_e \partial_{\xi} \hat{A}' = 0, \quad (5)$$

with an effective propagation constant  $\beta_e = \beta_0 + \beta_1(\omega - \omega_0)$ . This shows that the SEEA Eq. (2) accounts for the frequency dependence of diffraction as in a first-order dispersive medium. The SEWA envelope equation yields, however,  $\beta_e = \beta_0\omega/\omega_0$ , i.e., as in a nondispersive medium where all the frequencies travel at the the same velocity  $v_f$ . The paraxial diffraction Eq. (5) admits the Gaussian beam solu-

tion  $\hat{A}' = (-i\xi_R/q)\exp(i\beta_e r^2/2q)$ , where  $r = \sqrt{x^2 + y^2}$ ,  $q = \xi - i\xi_R$ , and  $\xi_R > 0$  is the Rayleigh range or diffraction length, which we take independent of frequency. The envelope spectrum is then

$$\hat{A} = \frac{-i\xi_R}{q} \exp\left(\frac{i\beta_e r^2}{2q}\right) \hat{\psi} \exp[(-\alpha_0/2 + i\hat{D})\xi], \quad (6)$$

where we have introduced an arbitrary amplitude  $\hat{\psi}$  for each frequency. Since the propagation constant is approximated, when concerned with diffraction effects, by the straight line  $\beta_e = \beta_0 + \beta_1(\omega - \omega_0)$ , it will take negative values for some frequencies, specifically for  $\omega < \omega_0 - \beta_0/\beta_1 = \omega_0(1 - v_g/v_f)$ , a frequency quite close to zero (exactly zero in the SEWA). To avoid these negative values of  $\beta_e$ , which lead to "anti-Gaussian" beams in the spectrum  $\hat{A}$ , and hence to "antibeam" behavior in the space-time domain, we shall take  $\hat{\psi} = 0$  for frequencies  $\omega < \omega_0(1 - v_g/v_f)$ . This condition does not entail a real restriction, since the lowest frequency  $\omega_0 - \Delta\omega/2$  in the frequency band  $[\omega_0 - \Delta\omega/2, \omega_0 + \Delta\omega/2]$  of pulses as short as a single period ( $\Delta t = T_0$ ) is sizeably higher than  $\omega_0(1 - v_g/v_f)$ . For example, the frequency band is about  $[0.75\omega_0, 1.25\omega_0]$  for a single-cycle pulse with a Gaussian-like spectrum  $\hat{\psi}$ , whereas  $\omega_0(1 - v_g/v_f)$  remains smaller than  $0.05\omega_0$  in the near-infrared and visible window of fused silica.

By inverse Fourier transform of Eq. (6), we obtain

$$A = \frac{-i\xi_R}{q} \exp\left(\frac{i\beta_0 r^2}{2q}\right) \left\{ \exp\left(-\frac{\alpha_0}{2}\xi\right) \frac{1}{2\pi} \int_{-\infty}^{\infty} d\omega \times \hat{\psi}(\omega - \omega_0) \exp(i\hat{D}\xi) \exp\left[-i(\omega - \omega_0)\left(\tau - \frac{\beta_1 r^2}{2q}\right)\right] \right\}. \quad (7)$$

The curly brackets can be identified with the solution  $\psi(\tau, \xi)$  of the SVEA equation

$$\partial_{\xi} \psi = (-\alpha_0/2 + iD)\psi, \quad (8)$$

with the initial condition  $\psi(\tau, 0)$  of spectrum  $\hat{\psi}(\omega - \omega_0)$ , but evaluated at the complex time  $\tau - \beta_1 r^2/2q$ . In conclusion,

$$A(r, \tau, \xi) = \frac{-i\xi_R}{q} \exp\left(\frac{i\beta_0 r^2}{2q}\right) \psi\left(\tau - \frac{\beta_1 r^2}{2q}, \xi\right) \quad (9)$$

satisfies the 3+1D SEEA Eq. (2) provided that  $\psi(\tau, \xi)$  satisfies the 1+1D SVEA equation for the same material medium, and represents a pulsed beam propagating under the joint effects of material gain (loss), phase and gain dispersion, diffraction, and space-time focusing. [The corresponding SEWA solution is obtained replacing  $\beta_1$  with  $\beta_0/\omega_0$  in Eq. (9).] The solution (9), henceforth referred to as the pulsed Gaussian beam (PGB), must satisfy condition (4) to be physically meaningful, no matter that  $\psi(\tau, \xi)$  breaks the SVEA being a single-cycle pulse.

The factor  $(-i\xi_R/q)\exp(i\beta_0 r^2/2q)$  in the PGB represents a Gaussian beam at the frequency  $\omega_0$  and diffraction length  $\xi_R$ . Its complex parameter  $q$  is usually expressed as [12]

$$\frac{1}{q(\xi)} = \frac{1}{R(\xi)} + \frac{2i}{\beta_0 a^2(\xi)}, \quad (10)$$

where  $R(\xi) = \xi[1 + (\xi_R/\xi)^2]$ ,  $a^2(\xi) = a_0^2[1 + (\xi/\xi_R)^2]$ , and  $a_0^2 = 2\xi_R/\beta_0$  are, respectively, the curvature radii of the phase fronts, the Gaussian width at each cross section  $\xi = \text{const}$  and the squared waist width. This Gaussian beam is modulated in the PGB by the SVEA pulse form  $\psi(\tau, \xi)$ , determining the on-axis pulse form of the PGB, but evaluation at a space-dependent complex time for off-axis points leads to some spatiotemporal coupling phenomena.

In vacuum ( $\alpha_0 = 0$ ,  $\beta_0 = \omega_0/c$ ,  $\beta_1 = 1/c$ ,  $D = 0$ ), Eq. (9) yields  $(-i\xi_R/\xi)\psi(\tau - r^2/2cq)\exp(i\omega_0 r^2/2cq)$ , with  $\psi(\tau)$  an invariant pulse form. This vacuum PGB has been recently shown to generate by mode-locking axial modes of stable laser resonators [9,8]. The transverse profile of the vacuum PGB is almost Gaussian, of width  $\approx a(\xi)$ , its form remaining invariant on propagation [8]. The vacuum PGB exhibits spatiotemporal coupling effects such as [8] pulse time delay, broadening, and redshift growing towards the beam periphery [8], these effects originating from the complex time shift  $r^2/2cq$ . In view of the PGB expression (9), these phenomena are qualitatively similar in material media. The diffraction-induced factor  $(-i\xi_R/q)$ , which introduces a phase  $\pi/2$  on propagation from  $\xi = 0$  to the far field, explains the observed polarity reversal [7] and time differentiation [5] of the on-axis pulse form  $\psi(\tau)$  on propagation. In dispersive media, this effect superimposes to the SVEA evolution  $\psi(\tau, \xi)$ .

#### IV. DIFFRACTION AND DISPERSION-INDUCED PULSE FRONT CURVATURES

The most significant spatiotemporal coupling phenomenon peculiar to dispersive pulsed-beam propagation is related to the curvature of the pulse fronts. The real part  $r^2/2v_g R(\xi)$  of the complex time is, both in vacuum and a dispersive medium, a diffraction-induced time shift of arrival of the pulse at each plane  $\xi$  for off-axis points. In space, this time shift results in an axial shift  $-r^2/2R(\xi)$  increasing quadratically with  $r$ , i.e., in paraxial spherical pulse fronts of radius

$$R_{DF}(\xi) = R(\xi). \quad (11)$$

The initially plane pulse front then becomes convex on propagation, by the same amount as the wave fronts of the Gaussian beam of the carrier frequency  $\omega_0$ . The physical explanation of this curvature is contained in the concept of space-time focusing. The redder frequencies, diffracted at larger angles, and therefore traveling at a reduced effective velocity, are delayed with respect to the bluer frequencies, diffracted at smaller angles.

In dispersive media we find an additional pulse front curvature in the PGB solutions of the SEEA equation, mathematically described through the imaginary part of the complex time  $\beta_1 r^2/\beta_0 a^2(\xi)$ , and physically originated by the difference of group velocities between the on-axis part of the pulse and the off-axis redshifted part. In normal dispersion, the red components, diffracted further from the axis, travel faster than blue components, nearer to the axis, while the opposite occurs in anomalous dispersion. Thus normal dis-

person originates a pulse front bending in the opposite sense to that of the diffraction-induced one. In anomalous dispersion, both curvatures add up.

For an initial ( $\xi = 0$ ) nearly transform-limited PGB in a lossless medium, the dispersion-induced pulse front curvature can be estimated as follows. Defining the redshift for off-axis points as

$$\delta = \frac{\int d\omega |\hat{A}|^2 (\omega - \omega_0)}{\int d\omega |\hat{A}|^2}, \quad (12)$$

using Eqs. (6) and (10), approximating  $\exp[-2\beta_1(\omega - \omega_0)r^2/\beta_0 a^2(\xi)] \approx 1 - 2\beta_1(\omega - \omega_0)r^2/\beta_0 a^2(\xi)$ , and taking into account that  $\omega_0 = \langle \omega \rangle = \int d\omega |\hat{\psi}|^2 \omega / \int d\omega |\hat{\psi}|^2$ , we obtain the expression  $\delta \approx -[2\beta_1 r^2/\beta_0 a^2(\xi)](\Delta\omega_{\text{rms}})^2$ , with  $(\Delta\omega_{\text{rms}})^2 = \langle (\omega - \omega_0)^2 \rangle$ . Since for a transform-limited pulse the rms duration and bandwidth are related by  $\Delta t_{\text{rms}} \Delta\omega_{\text{rms}} \approx 0.5$ , we get

$$\delta \approx -\frac{1}{2} \frac{\beta_1}{\beta_0} \frac{r^2}{a^2(\xi)} \frac{1}{(\Delta t_{\text{rms}})^2}. \quad (13)$$

The values of  $\delta$  are quite small in all cases; at the edge of the beam [ $r \approx a(\xi)$ ], and in the extreme case of a single-cycle pulse,  $\delta$  does not exceed  $0.1\omega_0$ .

On the other hand, the group velocity  $v_g(\omega) = [d\beta(\omega)/d\omega]^{-1}$  in a medium of propagation constant  $\beta(\omega) = \beta_0 + \beta_2(\omega - \omega_0) + \beta_2(\omega - \omega_0)^2/2 + \dots$  is given, for small shift  $\delta = \omega - \omega_0$ , by  $v_g(\delta) \approx v_g(1 - \delta\beta_2/\beta_1)$ .

Then the difference of axial distances  $v_g(\delta)t - v_g t$  traveled by the redshifted off-axis pulse and the on-axis pulse, at the instant  $t = \xi/v_g$  of arrival of the on-axis pulse at  $\xi$ , is given by  $-\delta\beta_2\xi/\beta_1$ . Introducing Eq. (13) for  $\delta$ , the dispersion length  $\xi_D = 2(\Delta t_{\text{rms}})^2/|\beta_2|$ , and the Gaussian beam relation  $\xi/a^2(\xi) = \xi_R^2/a_0^2 R(\xi)$ , we obtain an axial shift  $\pm \xi_R r^2/2\xi_D R(\xi)$ , with the plus and minus signs applying for normal ( $\beta_2 > 0$ ) and anomalous ( $\beta_2 < 0$ ) dispersion, respectively. This axial shift implies a pulse front curvature

$$R_{DS}(\xi) \approx \mp (\xi_D/\xi_R) R(\xi), \quad (14)$$

where the minus and plus signs stand for normal and anomalous dispersion, respectively.

The total curvature of the pulse fronts results from the superposition of the diffraction and dispersion-induced curvatures, and is estimated by

$$\frac{1}{R_T(\xi)} \approx \left(1 \mp \frac{\xi_R}{\xi_D}\right) \frac{1}{R(\xi)}. \quad (15)$$

In anomalous dispersion, the initially plane pulse fronts [ $1/R_T(0) = 0$ ] become on propagation more convex than in the nondispersive case. In normal dispersion the pulse fronts become convex or concave depending on whether diffraction is stronger ( $\xi_R < \xi_D$ ) or weaker ( $\xi_R > \xi_D$ ) than dispersion. If  $\xi_R$  is of the order of  $\xi_D$ , the pulse fronts will remain plane during propagation.

It is to be noted that the suppression of the pulse front curvature does not imply the elimination of the transversal

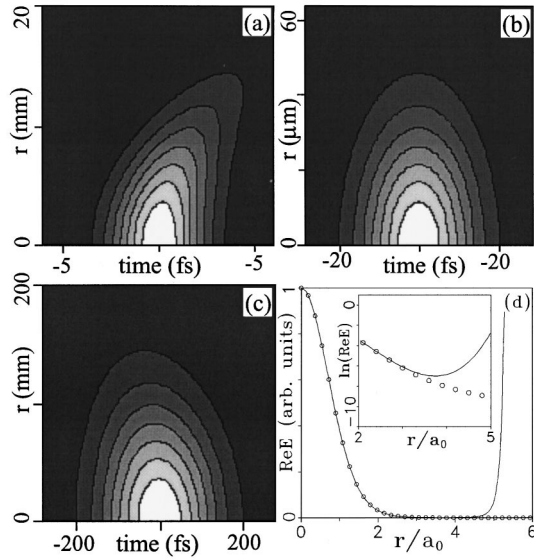


FIG. 1. Intensity ( $|A|^2$ ) contour plots of the propagated Gaussian PGB when (a)  $\xi_R < \xi_D$ , (b)  $\xi_R = \xi_D$ , (c)  $\xi_R > \xi_D$ . The numerical values of the parameters are given in the text. (d) Real field transverse profile of the Gaussian PGB (dots) and its approximation with the nontruncated Gaussian spectrum (solid line) at  $\xi=0$ ,  $\tau=0$ . The rest of the numerical values are those of case (b). The detail inside this figure shows the logarithm of the real field for a clearer comparison.

spreading due to diffraction. The PGB's in fact spread at the same rate as the monochromatic Gaussian beam of the carrier frequency, this rate being determined solely by the diffraction length  $\xi_R$ . In normal dispersion we can have, for example, an expanding beam with a concave pulse front.

### V. A PARTICULAR CASE: THE GAUSSIAN PGB

The previous results are confirmed by direct use of the PGB Eq. (9) in some particular cases. Figure 1 shows intensity contour plots of the propagated PGB of the initial Gaussian spectrum

$$\hat{\psi} = \sqrt{\pi} b_0 \exp[-b_0^2(\omega - \omega_0)^2/4], \quad (16)$$

weakly truncated for  $\omega < \omega_0 - \beta_0/\beta_1$  to ensure beam behavior. For conciseness, this particular SEEA solution will be called the Gaussian PGB.

In the three plots in Fig. 1, the carrier frequency is  $\omega_0 = 1.9 \text{ fs}^{-1}$ , the initial Gaussian pulse duration is  $b_0 = T_0/\sqrt{2\ln 2} = 2.8 \text{ fs}$  (which corresponds to  $\Delta t = T_0$ ), and the material parameters correspond to fused silica with GVD only, namely,  $\beta_0 = 9193 \text{ mm}^{-1}$ ,  $\beta_1 = 4881 \text{ mm}^{-1} \text{ fs}$ ,  $\beta_2 = 21.78 \text{ mm}^{-1} \text{ fs}^2$ , and  $\beta_i = 0$  for  $i > 2$ . The dispersion length is accordingly  $\xi_D = 2(\Delta t_{\text{rms}})^2/|\beta_2| = b_0^2/2|\beta_2| = 0.181 \text{ mm}$ . The only difference between Figs. 1(a), 1(b), and 1(c) is in the initial width,  $a_0 = 2, 6.3,$  and  $19 \mu\text{m}$ , respectively, to set the diffraction lengths to values smaller than, equal to, and greater than the dispersion length, namely,  $\xi_R = 0.1\xi_D, \xi_D,$  and  $10\xi_D$ . Note that for these values, the SEEA condition (4), which can now be expressed as [1]  $\beta_0\xi_D \gg 1, \beta_0\xi_R \gg 1$ , is met. The observation plane is always  $7\xi_R$ , where diffraction effects are well-developed.

The case of Fig. 1(a) ( $\xi_R = 0.1\xi_D$ ) can be assimilated to a nondispersive propagation, since diffraction is much stronger than dispersion. The pulse fronts are then convex (they appear concave in time). In Fig. 1(b) ( $\xi_R = \xi_D$ ), we see that dispersion has canceled the diffraction curvature. In fact, the pulse front remains plane during the whole propagation from  $\xi=0$  up to  $\xi \rightarrow \infty$ . Finally, in Fig. 1(c) ( $\xi_R = 10\xi_D$ ) the stronger dispersion turns the pulse fronts concave, in spite of the opposite effect of diffraction.

For the above Gaussian PGB, simple approximate analytic formulas can be obtained. Note first that as we move from the axis towards the beam periphery ( $r \rightarrow \infty$ ), the pulse spectrum  $\hat{A}$  shifts from  $\omega_0$  towards red frequencies, the truncation of the spectrum (at  $\omega \approx 0$ ) then becoming stronger. For the range of values of  $r$  for which the truncation remains small, the PGB with a nontruncated Gaussian spectrum (easier to handle analytically) is expected to reproduce accurately the true Gaussian PGB (with truncated spectrum). To estimate this range of  $r$ , we impose a redshift  $|\delta| < \omega_0$ , obtaining, according to Eq. (13),  $r^2/a^2(\xi) < 2\omega_0^2(\Delta t_{\text{rms}})^2$ . For an  $N$ -cycle pulse ( $b_0 = 2\Delta t_{\text{rms}} = NT_0/\sqrt{2\ln 2}$ ) the result is

$$r < \frac{N\pi}{\sqrt{\ln 2}} a(\xi) \approx 3.8Na(\xi), \quad (17)$$

a transversal distance substantially larger than the beam width  $\approx a(\xi)$ .

Consequently, we consider the SVEA equation (8) with GVD for the initial Gaussian spectrum (16) without truncation. The SVEA solution is the well-known Gaussian pulse [12]  $\psi(\tau, \xi) = (b_0^2/p)^{1/2} \exp(-\tau^2/p)$ , with  $p = b_0^2 - 2i\beta_2\xi$ . The pulse parameter  $p$  is often written in the form

$$\frac{1}{p(\xi)} = \frac{1}{b^2(\xi)} [1 + c(\xi)], \quad (18)$$

where  $b^2(\xi) = b_0^2[1 + (\xi/\xi_D)^2]$  and  $c(\xi) = [\text{sgn } \beta_2]\xi/\xi_D$  are the Gaussian pulse duration and chirp at any plane  $\xi = \text{const}$ . The corresponding PGB solution of the SEEA equation is obtained by replacing the real time  $\tau$  with the complex time  $\tau - \beta_1 r^2/2q$ , and by multiplying by the Gaussian beam of the carrier frequency:

$$A = \frac{-i\xi_R}{q} \exp\left(\frac{i\beta_0 r^2}{2q}\right) \left(\frac{b_0^2}{p}\right)^{1/2} \exp\left[-\frac{(\tau - \beta_1 r^2/2q)^2}{p}\right]. \quad (19)$$

This expression is still an exact solution of the SEEA Eq. (2), but lacks true beam behavior because of the frequencies  $\omega < \omega_0(1 - v_g/v_f)$  introduced. Figure 1(d) shows its transverse amplitude profile at  $\xi=0, \tau=0$  for a single-cycle pulse ( $N=1$ ). The amplitude grows without bound for large  $r$ ; however, it is virtually identical to the Gaussian PGB from  $r=0$  up to  $r$  between  $3a_0$  and  $4a_0$  (see the detail in logarithmic scale), as expected from Eq. (17). Similar results are obtained for other times and axial coordinates. Equation (19) thus provides a simple analytic expression for the Gaussian PGB valid at any position of space where the pulse amplitude is significant. Separating now the amplitude and phase factors in the last exponential of Eq. (19), and using the

expressions for the width, radius of curvature of the Gaussian beam, the duration, and chirp of the Gaussian pulse, Eq. (19) can be written, after long but straightforward algebra, in the following form:

$$A = \frac{-i\xi_R}{q} \exp\left(\frac{i\beta_0 r^2}{2q}\right) \left(\frac{b_0^2}{p}\right)^{1/2} \exp\left[-\frac{(\tau - \beta_1 r^2/2R_T)^2}{p}\right] \\ \times \exp\left[-i\delta\left(\tau - \frac{\beta_1 r^2}{2R_T}\right)\right] \exp\left[\frac{[1 - ic(\xi)]}{b_0^2} \frac{\beta_1^2 r^4}{\beta_0^2 a^4(\xi)}\right], \quad (20)$$

where  $R_T$  is given by Eq. (15) and  $\delta$  by Eq. (13) (with  $\Delta t_{\text{rms}} = b_0/2$ ). This expression explicitly shows that, for  $r < 3.8a$ , the Gaussian PGB has a Gaussian temporal form at any point of space, of duration  $b(\xi)$  and chirp  $c(\xi)$ , as the SVEA Gaussian pulse, and a complex amplitude that of the Gaussian beam of the carrier frequency. The last growing exponential in Eq. (20) modifies slightly the Gaussian complex amplitude, and becomes important only for large values of  $r$ , leading to the blow-up of the solution. Equation (20) also shows explicitly the redshift  $\delta$  of the oscillations within the envelope and the pulse front curvature  $1/R_T$ , whose magnitudes result to be exactly given by Eqs. (13) and (15) qualitatively derived in the preceding section.

## VI. CONCLUSIONS

To sum up, we have found a method to transform one-dimensional few-cycle solutions of the linear SVEA equation into three-dimensional solutions of the linear SEWA, or the slightly improved SEEA equation, incorporating in this way the effects of finite transversal size, diffraction (within the paraxial approximation), and first-order space-time focusing, together with the effects of gain and phase and gain dispersion of any order. The Gaussian PGB of Eq. (19) is the simplest example of these pulsed-beam waves in media with GVD, since it is written in the well-known terms of a monochromatic Gaussian beam coupled to a one-dimensional Gaussian pulse through the space-dependent complex time.

The most significant dispersion-diffraction coupling effect in the PGB solutions is the modification of the diffraction-induced pulse-front curvature with GVD, even its complete suppression when the dispersion and diffraction lengths are similar. From a practical point of view, this means the elimination of the pulse broadening due to diffractive pulse front distortion. One can easily understand this effect by thinking of diffraction as an anomalous dispersive phenomenon [13], since the red frequencies diffracted at larger angles advance slower than the blue frequencies, this anomalous dispersion being therefore dispensable with the proper amount of normal dispersion.

## ACKNOWLEDGMENT

This work was partially supported by the Comision Interministerial de Ciencia y Tecnologia of Spain (PB 95-0426).

- 
- [1] T. Brabec and F. Krausz, *Phys. Rev. Lett.* **78**, 3282 (1997).  
 [2] J. E. Rothenberg, *Opt. Lett.* **17**, 1340 (1992).  
 [3] J. K. Ranka and A. L. Gaeta, *Opt. Lett.* **23**, 534 (1998).  
 [4] Q. Lin and E. Wintner, *Opt. Commun.* **150**, 185 (1998).  
 [5] A. E. Kaplan, *J. Opt. Soc. Am. B* **15**, 951 (1998).  
 [6] I. P. Christov, *Opt. Commun.* **53**, 364 (1985).  
 [7] S. Feng, H. Winful, and R. W. Hellwarth, *Opt. Lett.* **23**, 385 (1998).  
 [8] M. A. Porras, *Phys. Rev. E* **58**, 1086 (1998). Note the opposite criterion of signs for the complex representation of monochro-

matic waves.

- [9] Z. W. Wang, Z. Zhang, Z. Xu, and Q. Lin, *IEEE J. Quantum Electron.* **33**, 566 (1997).  
 [10] E. Ibragimov, *Appl. Opt.* **34**, 7280 (1995).  
 [11] Z. Bor, *J. Mod. Opt.* **35**, 1907 (1988).  
 [12] See, for example, A. E. Siegman, *Lasers* (University Science, Mill Valley, CA, 1986).  
 [13] Diffraction has been in fact treated as such, including precursive effects, in E. M. Belenov and A. V. Nazarkin, *J. Opt. Soc. Am. A* **11**, 168 (1994).